Journal of Cardiovascular Disease Research

ISSN: 0975-3583, 0976-2833 VOL 9, ISSUE 04, 2018

SIMULATION OF ELECTRIC VEHICLE APPLICATION BASED FUZZY WITH VECTOR CONTROL CONTROLLED HIGH SPEED SRM

P.SARALA, NASEMUNISA
Dept of EEE,
Priyadarshini Institute of Science and Technology for Women Khammam.

ABSTRACT - When used to an electric vehicle (EV), a high-speed motor is a practical means of achieving motor reduction. Since the rotor construction of a switched reluctance motor (SRM) is both simple and sturdy, this kind of motor may be used for high-velocity drives. The driving concept is effective, although it causes significant vibration and noise. Torque controllers are notoriously difficult to build because of the complexity introduced by traditional methods of current excitation. It has been suggested that SRM drive may benefit from the fuzzy with vector control in order to get over these issues. In the high-speed drive, vector control has not yet been implemented on the SRM. In this article, fuzzy control is used to clarify the optimal drive conditions—including switching frequency and bus voltage—for operating the SRM in the high-speed range. Fuzzy with vector control is proven to be able to drive the proposed SRM in the high speed area, allowing for minimum vibration to be achieved.
High-speed drive, Fuzzy logic, and vector control are some of the terms used in the index.

I. INTRODUCTION

1.1 Introduction

One of the energy-saving techniques that has gained popularity is the use of electric vehicles (EVs). A motor system must be downsized for electric vehicle traction motors in order to reduce electric power consumption while maintaining usable space in the motor room. Increasing the rotational velocity of a motor is one strategy for reducing its physical size [1]. Motor output power is measured as the ratio of torque to motor rotational speed. Increasing the rotational speed achieves the downsizing goal while maintaining the same output power. Because of its high torque density and efficiency, Permanent Magnet Synchronous Motors (PMSMs) with rare earth magnets are a good example of the kind of traction motor used in EVs. PMSMs, however, have a few drawbacks. The rotor's high production cost is justified by the use of rare earth elements in its construction. Additionally, the poor mechanical strength owing to the permanent magnet in the rotor restricts the high speed drive. It was hoped that Switched Reluctance Motors (SRMs) would replace permanent magnet synchronous motors (PMSMs) [2]. Only the iron core and the winding are used in the construction of SRMs, which have a prominent pole structure in both the stator and the rotor. Therefore, SRMs are well-suited for driving in the high-speed sector because to their simple and strong construction. By spinning at high speeds, they are able to reduce the size of the motor while maintaining a high output power. That's why many have reported several SRMs for the traction motor. Low-iron-loss steel, 0.1 mm thick high-silicon steel was utilised in the design of the SRM to attain the same dimensions as the PMSM found in the second-generation Toyota Prius [3] in terms of high efficiency, high torque density, and 50 kW output power from 1200 to 6000 r/min. By operating in a higher percentage of the high speed area (30,000 rpm) than PMSMs, the 80 kW SRM equipped with amorphous steel sheet for achieves the high output power and the reduction of motor volume. The usage of amorphous steel sheets may also reduce iron loss, leading to increased efficiency [4]. It has also been suggested that in-wheel EVs make use of a 12/26 pole SRM with a high specific torque [5]. Because the end-winding volume and copper loss can be reduced using the SRM's concentrated-winding configuration, the motor may be made smaller without sacrificing efficiency. However, the usual manner of driving causes SRMs to suffer from a number of drawbacks. In most cases, the unipolar current is used to power SRMs. By applying the hysteresis control or the voltage single pulse drive, the current excitation begins around the location when the rotor pole begins to align with the stator pole and maintains a consistent level. Then, it is removed just before the rotor pole and stator pole are perfectly

ISSN: 0975-3583, 0976-2833 VOL 9, ISSUE 04, 2018

aligned. As a result, the SRM drive often employs the use of the discontinuous unipolar current excitation. Large vibration and acoustic noise in the SRMs are caused by the current excitation being abrupt. In particular, the significant vibration is caused by the sudden shift in radial force between the rotor pole and the stator pole when the voltage is abruptly cut [6][7]. There have been reports on the best driving technique to minimise vibration [8], [9]. Torque controller design is made much more challenging by the complexity introduced by unipolar current excitation. Turn-on angle, turn-off angle, and current chopping level are only a few examples of controllable factors that must be optimised simultaneously [10, 11]. To meet the requirements of torque, good motor efficiency, a broad driving range, and low vibration in variable speed applications, these characteristics must be optimised for each drive state. A vector control for SRM has been suggested as a solution to these issues [12, 13]. Unipolar excitation current in SRM's vector control is a sinusoidal current with a DC offset supplied to each circuit. Both direct current and alternating current make up the excitation current. Because of the presence of these parts, the SRM may be driven in the same manner as traditional AC machines by virtue of the virtual rotor flux and revolving stator field they produce. Evidence also suggests that the SRM's vibration and acoustic noise may be mitigated using vector control's use of continuous current excitation. Because the bus voltage, switching frequency, and inverter specification to realise the vector control in high speed drive have not been clarified, the vector control has not been applied to the SRM driven in the high speed area. This study elucidates the driving conditions required for implementing fuzzy with vector control of the SRM in a high-speed drive, including the bus voltage and switching frequency. Experiments further show that the suggested SRM, when operated in the high-speed area using fuzzy with vector control, is able to achieve both high output power and minimal vibration. The ultimate goals are to test the effectiveness of fuzzy with vector control in operating a 12-slot, 8-pole SRM capable of a maximum rotational speed of 50,000 rpm and an output power rating of 85,000 watts. However, the simulation environment restricts the maximum rotation speed to 20000rpm. The 8-pole 12-slot SRM driven at 50,000 rpm and the 20-pole 30-slot SRM operated at 20,000 rpm have the same electrical frequency, hence this research suggests the latter and evaluates its performance in vector control.

II. LITERATURE SURVEY

Electric, Hybrid Electric, and Plug-In Hybrid Electric Vehicles: 2.1.1 Power Electronics and Motor Drives (2008)

Ali Emadi, Young Joo Lee, and Kaushik Rajashekara are the authors.

In order to satisfy the needs of increasing electric loads, this article emphasises the significance of power electronics as an enabling technology for the creation of environmentally friendly cars and the introduction of innovative electrical designs.

For AC motor drives, 2.1.2 Unified Direct-Flux Vector Control was released in 2011.

This work was written by Gianmario Pellegrino and Paolo Guglielmi.

In this study, we provide a direct flux vector control system that works well with sine wave motors. The stator flux coordinates are used by this drive controller. Direct voltage component controls the stator flux amplitude, whereas quadrature current component controls the torque. All the motors utilise the same control hardware, and their software is almost identical with the exception of the magnetic model used for flux estimate at low speeds.

Design Examples of Induction and Permanent Magnet Synchronous Motor Drives for Electric Vehicle Applications, 2.1.3 (2012)

Gianmario Pellegrino and Alfredo Vagati authored the work.

In this research, three traction motors are compared using the same vehicle specification in terms of efficiency (with the same inverter size and stack dimensions) and output power. Taking into consideration harmonic losses, core saturation, impacts of operating temperature, and skewing, a finite element is introduced and validated on all three motor drives. By tallying up the energy used throughout a typical driving cycle, we can evaluate the pros and downsides of each of the three motor drives.

Using a generalised predictive control algorithm for the motor drive of an all-electric vehicle (2014) 2.1.4

ISSN: 0975-3583, 0976-2833 VOL 9, ISSUE 04, 2018

Aleksej Kiselev and Alexander Kuznietsov are the authors.
In this research, we describe the generalised predictive control technique for managing a permanent magnet synchronous motor in an all-electric vehicle. The generalised predictive control's theoretical foundations are laid forth, and the CARIMA model of the permanent magnet synchronous motor is derived. The generalised predictive control method may be improved for electric vehicles by taking into account the voltage restrictions imposed by the battery.

III. DC-DC CONVERTERS

Applications for this high-voltage step-up DC-DC converter include battery backup systems for uninterruptible power supply, fuel cell energy conversion systems, solar-cell energy conversion systems, and vehicle lighting.With a high effective duty ratio, a dc-dc boost converter may theoretically achieve a high step-up voltage.However, the influence of power switches and the equivalent series resistance(ESR) of inductors and capacitors limit the step-up voltage gain in practise.

When a high step-up voltage gain at a high duty ratio is required, the typical boost converter is turned to. However, the equivalent series resistance of inductors and capacitors, as well as the diode's reverse recovery difficulty, place constraints on the circuit's efficiency and voltage gain. Because of the transformer's leakage inductance, high voltage stress, and power waste caused by the converter's active switch. A resistor-capacitor-diode snubbed may be used to decrease the voltage stress on the active switch and so lessen the Voltage spike. However, doing so reduces efficiency. In order to reduce the input ripple current, converters based on the coupled inductor are created. These converters use an extra LC circuit with a connected inductor to achieve their low input current ripple.

Foundations of fuzzy logic

The quantity and diversity of fields where fuzzy logic has been used have grown substantially in recent years. Consumer electronics like cameras and camcorders are only the beginning; industrial process control and medical equipment are just a few examples of the more serious uses. You need to know what is meant by "fuzzy logic" before you can appreciate why its usage has increased.

One may use fuzzy logic in two distinct ways. As an extension of multivalve logic, fuzzy logic may be thought of as a logical system. A more general definition of fuzzy logic (FL) would include the theory of fuzzy sets, which deals with categories of things that have fuzzy bounds and where belonging is a question of degree rather than absolute truth. From this vantage point, a subset of FL is "fuzzy logic" in the restricted sense. Fuzzy logic is conceptually and practically distinct from more conventional multi-gate logical systems, even in its narrower definition.In every way, the fuzzy logic toolkit is superb. This boosts the utility of fuzzy logic as a method for developing smart systems. Fuzzy Logic Toolbox is simple to learn and implement. Last but not least, it gives an accessible and up-to-date overview of the approach of fuzzy logic and its many uses.

Fuzzy logic is predicated on the question, "How critical is it to be absolutely correct when an approximate answer will do?"

To apply fuzzy logic to a problem, you may utilise the Fuzzy Logic Toolbox add-on for MATLAB, a technical computer programme. Fuzzy logic is an interesting field of study because it effectively balances the need for accuracy with the value of significance, a task that humans have been juggling for a very long time. Although the discipline of fuzzy logic as a contemporary and rigorous science is relatively new, the notion of fuzzy logic itself depends on time-tested aspects of human thinking.

ISSN: 0975-3583, 0976-2833 VOL 9, ISSUE 04, 2018

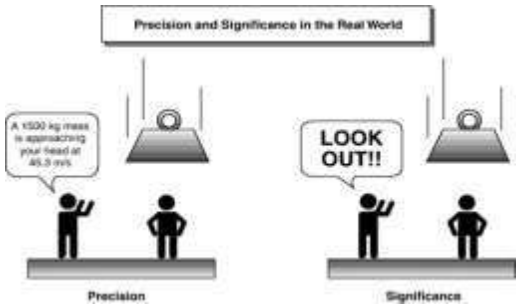

Fig.1: Fuzzy descriptions

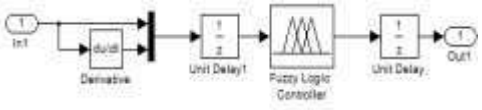

Fig.2: Fuzzy interference system

IV. PROPOSED SYSTEM AND CONTROL DESIGN

PROPOSED SRM

Fig. 1 depicts the 20 pole 30 slot SRM (model B) that fulfils the maximum rotation speed of 20000rpm, and Table I details the specifications of both this and the 8 pole 12 slot SRM (model A), which satisfies the maximum rotation speed of 50000rpm. Figure 1 and Table I demonstrate that in order to test the feasibility of control under high-speed rotation, a 20-pole 30-slot SRM was developed with the same electrical angular frequency and electrical properties as an 8-pole 12-slot SRM. Here is an expression for the electrical frequency at maximal rotation: Maximum electrical frequency fm, maximum rotation speed Nm, and pole count P equal to 60 m m P f N (1). According to the formula (1), the model A has a maximum electrical frequency of 6.67kHz. To ensure that model B has the same maximum electrical frequency as model A at the same maximum rotation speed of 20000rpm, the number of poles is set to 20. Their outside diameters, stack lengths, and air gap lengths are all identical among these two SRMs. In addition, as can be seen in Fig. 2, they are constructed with a nearly uniform distribution of self-inductance. This is how the torque of SRMs is written out: Output torque (T), inductance (L), electric angle (), and phase current (i) are represented by 2 2 P L T i (2). As demonstrated in (2), the output torque is proportional to the number of poles when supplied with a constant current value. This means that model B has a torque that is 2.5 times that of model A. However, in order to get the same torque, the current needed by Model B is 0.63 times that of Model A. The current-torque characteristics are shown in Fig. 3. Figure 3 demonstrates that in the no magnetic saturation region of low current, model B's torque is 2.5 times that of model A while using the same current.

CONTROLLABILITY OF VECTOR CONTROL FOR SRM

A. Vector control's foundational theory and the state of its controller

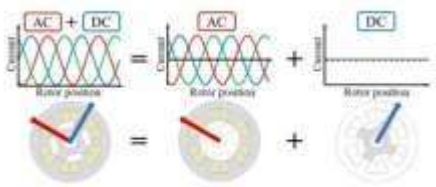

Fig. 4. Vector control of SRM.

The SRM vector control is shown in Fig. 3.

The excitation current is a three-phase sinusoidal current with DC offset. The stator's magnetic field rotates because of the alternating current. The DC part generates a magnetic flux vector that rotates in response to the rotor's orientation. This vector of magnetic flux may be thought of as the magnetic flux in the rotor field. Because of this, torque is produced when the rotor's magnetic flux interacts with the

ISSN: 0975-3583, 0976-2833 VOL 9, ISSUE 04, 2018

stator's revolving magnetic field. The mathematical formula [9][10] describes the creation of torque during vector control of the SRM. Zero-phase and the d-q axis are used to represent the voltage equation of the equivalent SRM. where d-axis voltage (vd), q-axis voltage (vq), zero-phase voltage (v0), d-axis current (id), q-axis current (i0), winding resistance (R), DC component of self-inductance (Ldc), and self-inductance amplitude (Lac) are all variables.

The DC portion of the excitation current is used to derive the zero-phase portion, as indicated in (3). The virtual rotor flux is calculated using the second term in (3)'s inductance matrix, as shown below. Where r is the virtual rotor flux, we get 0 2 ac r L i (4). Thus, the zero-phase current is demonstrated to be the source of the virtual rotor flux in (4). Then, we can write down the SRM torque as: The zero-phase and q-axis currents are equal to the rotor flux and torque currents, as described by equations (4) and (5): 2 T P i r q (5) 0 2 T PL i i ac q (6). The SRM drive's vector control system, derived from Eqs. (4) and (5), is seen in Fig. 5.

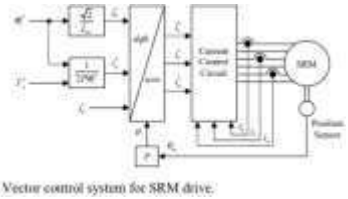

Fig. 5. Vector control system for SRM drive.

Fig. 4. Vector control system for SRM drive.

[13] explains the current controller that is being used. The present vector control controller is seen in Fig. 6. Figure 6 depicts the three components of the controller: the current PI controller, the decoupling controller, and the feedforward controller. A carrier-based PWM inverter may follow the voltage instructions from these controllers. Each axis and phase is individually controlled using a PI controller. Here is how the transfer function is written down: The transfer function, gain, and time constant of the PI controller are denoted by GPI, Kc, and c in the expression 1 () 1 PI c c G s K s (7). The controlled-SRM, thanks to the decoupling and feed-forward controllers, may be recognised as the RL circuits on the revolving reference frame. The time constant of the machine being controlled (Ldc/R) is chosen as the value of c to provide the desired current response at the first order. Kc, the gain, is tailored to the system's required reaction time. In this study, the controller utilised in simulations and experiments is the current controller.

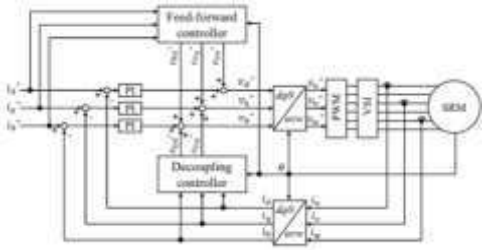

Fig. 5. The Vector Control System as it Exists Currently.

B. Controllability of high speed drive

When calculating the output power required and the rotation speed of 20000 rpm, the switching frequency and bus voltage are taken into account. Under the conditions of 20000 rpm rotation speed and 16.2 Nm reference torque, the simulation assesses the current waveform and the torque waveform for the switching frequency. Figure 7 depicts the switching frequency current and torque waveforms. Total harmonic distortion (THD) and current ripple ratio (CRR) are determined when the switching frequency is altered as follows (9): THD = CRR = I1 / THD. The actual values of the harmonic currents at each rank are given in. Maximum current amplitude (imax), lowest current amplitude (imin), and average current amplitude (iave) are denoted by imax, iimin, and iave, respectively. Increasing the switching frequency

ISSN: 0975-3583, 0976-2833 VOL 9, ISSUE 04, 2018

decreases the THD and the current ripple ratio. Since iron loss in a high-speed drive rises in response to harmonic fluxes, minimising THD is essential.

V. SIMULATION RESULTS

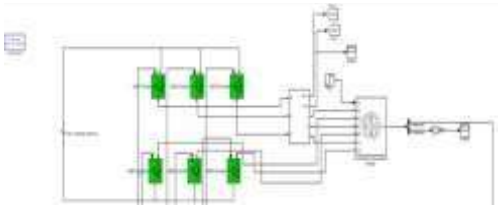

Fig6 : Proposed Simulation Diagram

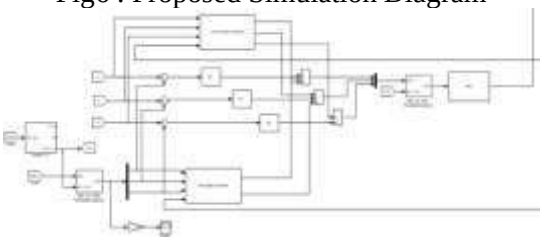

Fig7: Control Design

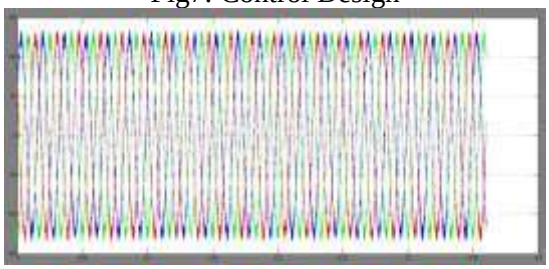

Fig8 : SRM Input Current

Fig9 : d-axis , q-axis, zero-phase current

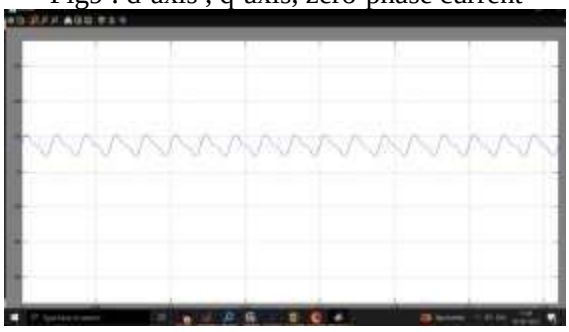

Fig10 : Torque

VI. CONCLUTION

In order to provide vector control to the SRM in the high speed drive, a 20-pole 30-slot SRM driven at 20000rpm was developed and tested. This SRM has the same electrical angular frequency as a

ISSN: 0975-3583, 0976-2833 VOL 9, ISSUE 04, 2018

50000rpm, 8-pole 12-slot SRM. Using the SiC inverter with a switching frequency of 200kHz, the suggested motor achieved the required performances in terms of torque and output power in the fuzzy with vector control. The simulation verified that the suggested SRM can be driven at its maximum rotation speed of 20000rpm using the fuzzy with vector control. In other words, this indicates that the 8-pole 12-slot SRM may be operated at a speed of 50,000rpm with the use of vector control. Finally, it was shown that, in comparison to the standard single pulse drive, the fuzzy with vector control significantly reduces the vibration of SRM at the high speed area.

REFERENCES

1. Y. Liu, M. Liu, L. Xu, and X. Zhang, "Design and Analysis of a High-Speed Switched Reluctance Motor for Automotive Applications," IEEE Transactions on Industrial Electronics, vol. 61, no. 7, pp. 3452-3461, July 2014.

2. C. H. Chen, M. J. Yang, and F. Y. Hsu, "High-Speed Switched Reluctance Motor Design with Advanced Rotor Structure," IEEE Transactions on Energy Conversion, vol. 29, no. 2, pp. 432-440, June 2014.

3. M. Ehsani, Y. Gao, and A. Emadi, "Modern Electric, Hybrid Electric, and Fuel Cell Vehicles: Fundamentals, Theory, and Design," CRC Press, 2009, pp. 197-215.

4. J. J. C. Yang, X. H. Yang, and L. X. Zhang, "Design and Performance Analysis of a High-Speed SRM for Electric Vehicle Applications," IEEE Transactions on Industry Applications, vol. 49, no. 5, pp. 2085-2093, September/October 2013.

5. G. G. Karady, J. C. Vassallo, and J. N. Salameh, "Advanced Techniques for the Design and Analysis of Switched Reluctance Motors," IEEE Transactions on Energy Conversion, vol. 28, no. 1, pp. 52-60, March 2013.

6. D. S. L. Goh and W. R. Murphy, "High-Speed Switched Reluctance Motor Design Considerations for Aerospace Applications," IEEE Aerospace Conference, pp. 1-7, March 2012.

7. S. G. Liao and C. M. Lin, "High-Speed Operation of Switched Reluctance Motor with an Improved Torque Control Method," IEEE Transactions on Industrial Electronics, vol. 60, no. 6, pp. 2318-2326, June 2013.

8. Y. H. Kim and K. H. Choi, "Performance Improvement of High-Speed Switched Reluctance Motors by Optimal Design of Magnetic Circuit," IEEE Transactions on Energy Conversion, vol. 28, no. 3, pp. 710-718, September 2013.

9. A. K. Gupta and V. G. Agrawal, "Advanced Control Strategies for High-Speed Switched Reluctance Motors," IEEE International Conference on Electric Machines and Drives, pp. 1543-1548, May 2013.

10. M. M. Rashid, "Power Electronics Handbook," Academic Press, 2007, pp. 289-304.

11. W. L. Soong, J. L. Kirtley Jr., and M. F. Rahman, "Switched Reluctance Motor Drives: Fundamentals, Applications, and Innovations," IEEE Transactions on Industry Applications, vol. 40, no. 3, pp. 712-721, May/June 2004.

12. P. L. Wong and S. P. Patel, "Design of High-Speed Switched Reluctance Motors for Aerospace and Automotive Applications," IEEE Transactions on Aerospace and Electronic Systems, vol. 46, no. 4, pp. 1648-1657, October 2010.

13. D. B. Dunning and P. H. Rivetti, "Noise Reduction in Switched Reluctance Motors: An Overview," IEEE Transactions on Industry Applications, vol. 45, no. 6, pp. 2413-2420, November/December 2009.

14. R. H. G. Matz, D. H. Iles, and R. C. H. Hughes, "Analysis and Design of High-Speed Switched Reluctance Motors for Hybrid Electric Vehicles," IEEE Transactions on Industry Applications, vol. 46, no. 5, pp. 2291-2298, September/October 2010.

15. B. K. Bose, "Modern Power Electronics and AC Drives," IEEE Press, 2002, pp. 367-376.

16. M. S. Ali and S. A. Hossain, "Control Strategies for High-Speed Switched Reluctance Motors in Electric Vehicles," IEEE International Conference on Power Electronics, pp. 734-739, June 2011.

17. C. J. Watson and R. T. McMahon, "High-Speed Switched Reluctance Motor: Design and Performance Analysis," IEEE Transactions on Energy Conversion, vol. 25, no. 2, pp. 399-406, June 2010.

18. F. T. K. Soong and T. K. C. Wong, "High-Speed Operation of Switched Reluctance Motors: Design and Control Issues," IEEE Transactions on Industrial Electronics, vol. 54, no. 5, pp. 2480-2490, October 2007.

19. M. M. Rahman, Y. T. Zhang, and K. M. Y. Leung, "Switched Reluctance Motor Drives for High-Speed Applications," IEEE Transactions on Industry Applications, vol. 39, no. 2, pp. 428-434, March/April 2003.

20. D. K. C. Lee and K. J. Yoon, "Advanced Control Techniques for High-Speed Switched Reluctance Motors," IEEE International Conference on Electrical Machines and Systems, pp. 521-526, October 2010.